Improved AVA imaging in laterally varying media

Wim J.F: van Geloven and C.P.A. Wapenaar, Delft University of Technology*

Summary

When a wave propagates through a bed of thin layers, its reflection is accompanied by wavelet interference. These interference effects are also dependent on the angle of incidence of the wave. Due to the bandlimitation of the seismic data, these interference effects cannot be removed. However, by the application of a spatial bandlimitation filter, these interference effects can be equalized. This method was already tested for one-dimensional inhomogeneous media. We give here an extension of this method to two- and three-dimensional inhomogeneous media.

Introduction

Amplitude-Versus-Angle (AVA) inversion is normally done using Zoeppritz equations. However, it is well known that the relation between the AVA-effects, present in seismic data, and the angle-dependent reflectivity becomes complicated, when the layer thicknesses become smaller than half the wavelength. In that case it is no longer justified to consider the individual reflecting boundaries as being isolated [1]. Because of this, the Zoeppritz equations predict different AVA-behaviour than present in the seismic data.

To alleviate this problem Wapenaar et al. [2] introduced an improved imaging procedure that equalizes correctly for the apparent AVA-behavior. However, in that paper only one-dimensional media were discussed. In this paper we will give an outline of the extension of this method to two- and three-dimensional inhomogeneous media. First we will discuss the filter that will be applied to the downward extrapolated data. Then we will describe how this filter will be incorporated in the process of migration. In this process we also bring into account the local dip of the finely layered structure, given that some information about this dip is known in advance.

Apparent AVA effects due to fine-layering

The apparent AVA-effects due to fine-layering can be subdivided into propagation and reflection related effects. The propagation through a package of thin layers is accompanied with angle dependent wavelet *dispersion.* This has been extensively discussed in previous papers and it will not be further considered here. The reflection of a package of thin layers is accompanied by wavelet *interference.* This interference effect depends on the angle as well. This can be explained with the aid of Figure 1. In this picure two plane waves are shown that illuminate a horizontally layered medium under two different angles. The circular frequency ω of the two waves is chosen the same. We can see that the vertical wavelength λ_z differs for both waves. In other words, we can say that for different illumination angles, the medium is observed by the two waves with different gauges. This implies that the interference effects are different for distinct angles, which

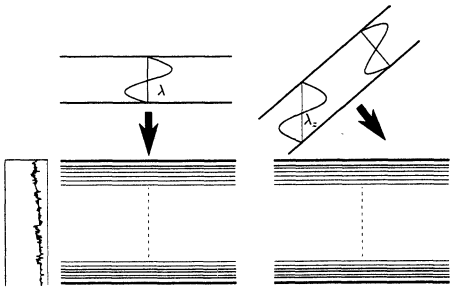

***Fig.** 1: Horizontally layered medium: Different angles ϕ, same angular frequency w*

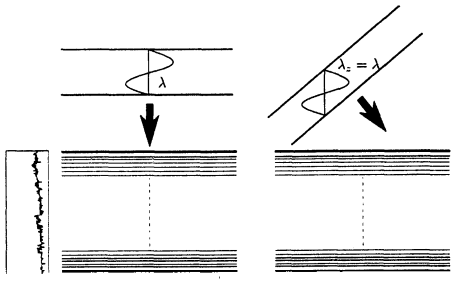

***Fig.** 2: Horizontally layered medium: Different angles ϕ, same vertical wavelength λ_z*

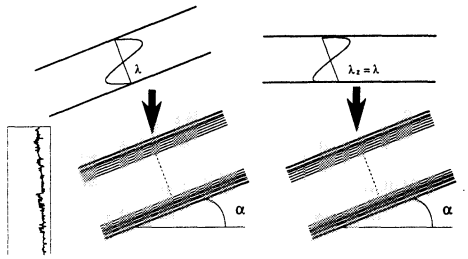

***Fig. 3:** Layered medium with a dip α: Different angles ϕ, same wavelenght λ_n*

is the case for apparent AVA. To alleviate this problem, we take plane waves with different frequencies in such a way that the vertical wavelength λ_z stays constant, as can be seen in Figure 2. Furthermore, if the finely layered medium has a dip α (see Figure 3) we have to keep the wavelength constant in a line perpendicular to the boundaries of the medium. We will call this particular wavelength λ_n, where *n* stands for the normal direction, perpendicular to the layers. For a constant velocity medium with velocity c, the circular frequency ω and the normal wavelength λ_n are related as,

$$\lambda_n = \frac{2\pi c}{w \cos(\phi - a)}, \qquad (1)$$

where

$$\phi = \arccos(\sqrt{1 - c^2 p^2}). \qquad (2)$$

In this equation p is the horizontal ray-parameter. In order to keep the normal wavelength equal, we have to keep the factor w cos $(\phi -$ a) constant. Therefore, in the downward extrapolated wavefield only that data is used, for which the normal wavelength can be kept equal.

An illustration of this procedure can be found in Figure 4. The upper frame of this figure depicts the result of a downward extrapolation in the p, w-domain with all frequencies present. In the figure $p = 0$ corresponds to $\phi = \alpha$. In the lower frame, only those frequencies (in the relevant seismic frequency-band) are included, that have constant spatial bandwidth. In other words, only that data is kept that is located between two lines of constant λ_n. The objected result is shown in Figure 5, where we have depicted two AVA-curves of a cross-section, *without* and *with* the filter. It will be clear that the apparent AVA effects have been removed completely when the filter has been applied. In the following section we will outline how this filter will be applied to two- and three-dimensional varying media.

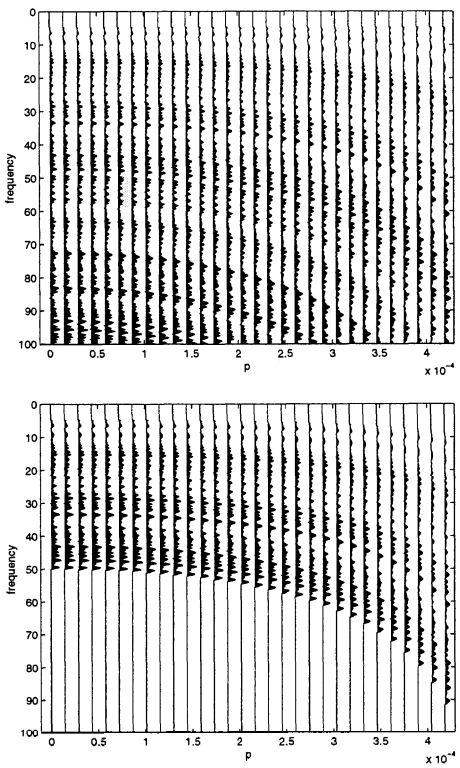

Fig. 4: Upperframe: downward extrapolated data with constant temporal bandwidth; lower frame: filtered data with constant spatial bandwidth

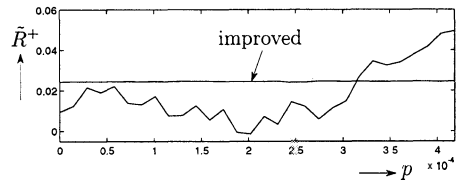

***Fig. 5: Example** of an amplitude cross-section, without (dashed) and with (solid) filter applied. Since we consider a density contrast the reflectivity is angle independent*

True amplitude angle-dependent migration

First we will describe the model, which is shown in Figure 6. At the target zone a finely layered structure is located. Above this structure we may have an arbitrary overburden. Locally the structure may be viewed as a stack of parallel layers, which is tilted with an angle α. Note that this limits the total thickness of the stack. The depth levels of the layers may then locally be described by the function

$$z'(\mathbf{x}, \alpha, z_i) = -\tan(\alpha) \,.\, \mathrm{x} + z_i. \qquad (3)$$

We model the reflection response in the space-frequency domain as follows,

$$P^-(\mathbf{x}_R, \mathbf{x}_S, \omega) = \int_\Omega W^-(\mathbf{x}_R, \mathbf{x}, \omega) \hat{R}^+(\mathbf{x}, \omega) W^+(\mathbf{x}, \mathbf{x}_S, \omega) S(\omega) d^3\mathbf{x}, \qquad (4)$$

where $\mathbf{x}_S$ and $\mathbf{x}_R$ denote the source and receiver coordinates, respectively. W^+ (x, $\mathbf{x}_S$, w) and W^- ($\mathbf{x}_R$, x, ω) are the two- of three-dimensional propagators for downgoing and upgoing waves, which are mutually related, ac-

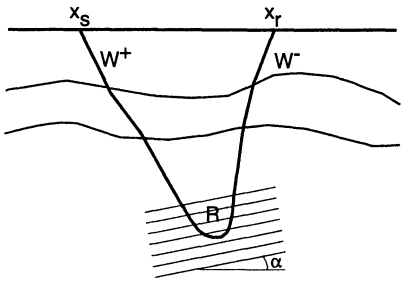

Fig. 6: Model of the subsurface, with a finely-layered medium at a depth z_α

cording to $W^-(\mathbf{x}_R, x, \omega) = W^+(\mathbf{x}, \mathbf{x}_R, \omega)$. Finally, $\hat{R}^+(x, \omega)$ is the reflection operator; the hat ($\hat{}$) denotes that it is a pseudo-differential operator. Its kernel reads $R^+(\mathbf{x}_H, z; \mathbf{x}'_H, w)$, where $\mathbf{x}_H = (x, y)$.

Following the lines of [2] we now propose an extension to a two- and three-dimensional imaging method. Suppose we know the result of a downward extrapolation to the (tilted) depth level z' that reads $P^-(\mathbf{x}_H, z'; \mathbf{x}'_H, z', w)$. After a Radon transform along the tilted "offset coordinates" $\mathbf{x}_H - \mathbf{x}'_H$ at depth level z' we obtain $\tilde{P}^-(\mathbf{p}, z'; \mathbf{x}'_H, z', \omega)$, where $\mathbf{p} = (p_x, p_y)$, p_x and p_y being the ray-parameters in the x- and y-direction. In analogy with the equations in the above mentioned reference we write for the imaged reflection kernel in the Radon domain

$$\langle \tilde{R}^+(\mathbf{p}, z'; \mathbf{x}'_H) \rangle = \frac{2 \cos \bar{\phi}(\mathbf{p}, z'; \mathbf{x}'_H)}{\pi \bar{c}(\mathbf{x}'_H, z)} \Re \int_{\omega_1(z')/\cos\bar{\phi}(\mathbf{p},z;\mathbf{x}'_H)}^{\omega_2(z)/\cos\bar{\phi}(\mathbf{p},z;\mathbf{x}'_H)} \left(\frac{\tilde{P}^-(\mathbf{p}, z'; \mathbf{x}'_H, z', \omega)}{S(\omega)} \right) d\omega, \quad (5)$$

where

$$\cos \bar{\phi}(\mathbf{p}, z'; \mathbf{x}'_H) = \sqrt{1 - \bar{c}^2(\mathbf{x}'_H, z')|\mathbf{p}|^2}. \quad (6)$$

For each $\mathbf{x}'_H$, $\langle \tilde{R}^+(\mathbf{p}, z'; \mathbf{x}'_H) \rangle$ represents an angle-dependent reflectivity section without apparent AVA, assuming the medium is locally parallel layered at $(\mathbf{x}'_H, z')$. The integration interval of equation (5) replaces the filter as discussed in the previous section. Furthermore, note that in the equations (5,6) the velocity medium is assumed locally homogeneous. At each imaged point $(\mathbf{x}'_H, z')$ the velocity c is replaced by the local macro model velocity $\bar{c}$.

As an example, Figure 7 shows the reflectivity sections and corresponding AVA-curves of a reference section, the

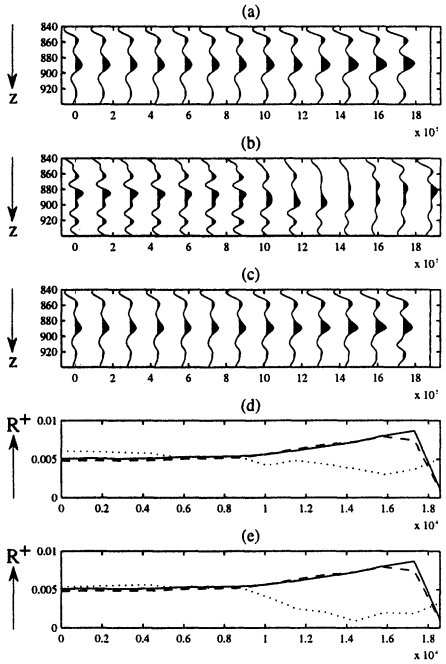

Fig. 7: Example of a reflectivity section: (a) reference section, (b) unfiltered migration result, (c) filtered migration result, (d) picked amplitude in a band of ± 10 meters, (e) picked amplitudes at the exact location [(a) solid, (b) dotted, (c) dashed]

result of migration without and the result of migration with the spatial bandlimitation filter. It will be clear that reflection related apparent AVA-effects are equalized by the new method of filtering. Futhermore we can see from this example that the image of the boundary is much better localized. The results of Figure 7 have been obtained for a horizontally layered overburden. Similar results for a laterally varying overburden will be discussed during the presentation.

Conclusions

We have discussed an extension to a method that compensates for the reflection related AVA-effects. This method was already proven, within the used modelling method, for one-dimensional inhomogeneous media. In this paper, we have given an outline how to develop this method further for two- and three-dimensional inhomogeneous media. Apart form this development, we plan to integrate this imaging method in a multidimensional migration scheme that accounts for the related propagation AVA-effects as well.

Acknowledgement

The work reported here was supported under a grant from the Dutch Science Foundation STW (DTV 44.3547)

References

[1] Ostrander, W.J., Plane-wave reflection coefficients for gas sands at nonnormal angles of incidence: Geophysics 49, 1637-1648,1984

[2] Wapenaar C.P.A., T.S. van der Leij & A.J. van Wijngaarden, AVA and the effects of interference: 65th Ann. Internat. Mtg. Soc. Expl. Geophys., Expanded Abstracts, Soc. of Expl. Geophys., 1125-l 128, 1995

[3] Van Wijngaarden, A.J. and C.P.A. Wapenaar, Resolution Analysis in linearized elastic inversion: 65th Ann. Internat. Mtg. Soc. Expl. Geophys., Expanded Abstracts, Soc. of Expl. Geophys., 647-650 , 1995